

PRODUCTION CHARACTERISTICS INVESTIGATION OF NATURAL GAS HYDRATE BY COMBINATION METHOD OF THERMAL STIMULATION AND WATER FLOW EROSION IN MARINE SEDIMENT

Bingbing Chen¹, Huiru Sun¹, Dayong Wang¹, Yongchen Song¹, Mingjun Yang^{1*}

1 Key Laboratory of Ocean Energy Utilization and Energy Conservation of Ministry of Education, Dalian University of Technology, Dalian, 116024, PR China

ABSTRACT

Natural gas hydrates (NGHs) are considered as an alternative and potential energy. Three classes of NGHs deposits are classified according to the layers present around. Studies on appropriate method for different classes of NGHs deposit was extremely important. Considering the huge seawater source, and its higher temperature than the hydrate deposit, the combination mode of seawater flow erosion and thermal simulation was investigated in this study. The results indicated that the combination mode will provide great driving force for methane hydrate (MH) decomposition with the higher temperature and higher seawater flow velocity. Via the combination mode, there are three obvious stages for hydrate decomposition: a) water saturation; b) residual gas displacement and sudden hydrate formation/decomposition; c) continuous hydrate decomposition. What's more, the seawater flow process has more obvious promotion effect for hydrate decomposition than temperature increase, due to the plenty heat-loss. In short, the huge seawater source has already decided the great potential of this combination method for actual hydrate production.

Keywords: natural gas hydrate, marine sediment, production characteristics, seawater flow erosion, thermal stimulation,

1. INTRODUCTION

Natural gas hydrates (NGHs) are considered as an alternative and potential energy, due to its characterizes of clean, high energy density and wide distribution [1, 2]. How to achieve the safe and efficiency recovery of NGHs has become the research hotspot around the world [3].

Three classes of NGHs deposits are classified according to the layers present around [4]. Both class 1 and class 2 contain a hydrate layer and an underlying free water zone [5]. Class 3 only contains a hydrate layer without any underlying and overlying fluid layer [6]. It is more important to choose an appropriate method for different classes of NGHs deposit [7].

As reported, pressurization, thermal simulation, water flow erosion and their combination methods have been proved the validity for NGHs recovery [8, 9]. Among these production method, thermal simulation is one of the widely discussed method [10]. However, the disadvantage of thermal simulation of lower heat utilization and higher costs caused the low NGHs production efficiency [11]. What's more, water flow erosion has also been proved to be a potential and efficiency method for NGHs production based on the water-gas migration in hydrate sediment [12-14]. Therefore, considering the huge seawater source with higher temperature than the temperature of hydrate layer, the combination mode of water flow erosion and thermal simulation has huge potential and necessary to be further studied. Especially, the thermal simulation method could firstly induce the hydrate decomposition at local areas, which will further improve the permeability of seawater.

So, based on this, the combination mode of seawater flow erosion and thermal simulation was first investigated in this study.

2. EXPERIMENT

2.1 Apparatus and materials

The detailed description about apparatus can be found in our previous works [13]. The schematic of experimental setup is shown in Fig. 1. Briefly, a high-pressure vessel (effective size is 15*200 mm the stand pressure is 15 MPa), made of nonmagnetic material, was used to form and decompose MH. Three high-pressure syringe pumps (260D) were used to control the water flow process, the inner pressure of vessel and gas injection. An MRI system (operating at 400 MHz) was used to directly observe the aqueous phase distribution in porous media during the whole experiment. A standard spin echo pulse sequence was chosen to obtain the 2D proton density weighted images. The time interval of this sequence was 2 minutes. Three thermostat baths filled with fluorinert (FC-40) was used to control the temperature of water, gas, vessel, respectively. The differential pressure of the hydrate-saturated sand core was measured by two Rosemount smart pressure transducers (± 0.1 MPa), which were connected to the input and output of the vessel. The signals of temperature and pressure are collected by A/D module (Advantech Co., Ltd., Taiwan, China). BZ-02 glass beads (porosity 35.4%, 0.177-0.250 mm) were packed into vessel and used to simulate the hydrate reservoir. Deionized water was used to configure the seawater.

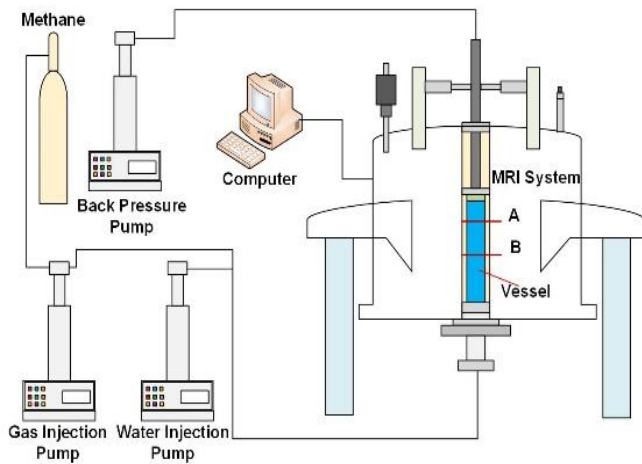


Fig 1 Schematic of experimental setup

2.2 Experimental procedure

The dry glass beads were tightly packed into the vessel. After 20 mins vacuuming, the denoised water was injected into the vessel with a gradually increased pressure, and keep stable for 1 h when the pressure reached 6000 kPa. Then, the output valve was opened to make the inner pressure of vessel reach atmospheric pressure. MH was injected into vessel with a constant pressure of 4000 kPa to displace pore-water. The volume

of injection water and displaced water were recorded to calculate the initial hydrate saturation. After that, the vessel was pressurized 6000 kPa with CH_4 and kept stable during MH formation process. The temperature of sediment was always kept at 274.15 K during the whole experiment process. No obvious gas consumption reflected the completeness of MH formation process. Then, the inner pressure of vessel was dropped to 3200 kPa, which still higher than the equilibrium pressure of 2850 kPa. Finally, the seawater was continuously injected into the hydrate-bearing sand sample with a constant rate of 2 mL/min and 10 mL/min, respectively. Meantime, the temperature of seawater was controlled to 275.15 K and 277.15 K, respectively. The entire experiment process was continually recorded by MRI with a constant interval of 2 Mins. The details of the experimental conditions and parameters are shown in Table. 1.

Table 1. Experimental parameters.

Case	v/mL/min	T_w /K	$S_{hi}/\%$	P_b /kPa	P_e /kPa
1	2	275.15	30.46	3200	3150
2	2	277.15	30.67	3200	3800
3	10	275.15	29.23	3200	3150

^a The symbols in this table are defined as follows: V is the water flow rate; T_w is the temperature of flowing seawater; S_{hi} is the initial MH saturation before hydrate decomposition (volume fraction); P_b is the backpressure during seawater flow process; P_e is the equilibrium pressure corresponding to T_w .

3. RESULTS AND DISCUSSION

3.1 Hydrate formation

MRI has been widely used to visually investigate hydrate formation and decomposition [15]. Fig. 2 shows the mean intensity (MI) and water saturation distribution variations during hydrate formation. In figures, the color of red and green represent free water signal value, red reflects higher signal value than green. Blue represents the gas and methane hydrate, the darkened blue reflects the lower free water saturation and higher methane hydrate saturation.

As shown in Fig. 2, there was four stage for hydrate formation. For stage I, there was no hydrate formation at the initial stage. Then, the hydrate formed rapidly in local area, as evidently seen from the MRI image (stage II). Meantime, the MI showed a significant decrease trend, due to the consumption of free water. After that, there will be a plenty of hydrate formation in the entire sand sample. As shown in MRI image (stage III), the darkened blue distributed in most regions and the MI appeared to

continuously decrease trend. Due to the impermeability of hydrate, the hydrate distributed in inlet region prevent the methane gas migration and further decrease the hydrate formation rate. Thereby, the MI showed a relative stability trend from 150 mins to 360 mins. Finally, for stage IV, the entire field of view (FOV) showed darken blue at 1200 mins. Meanwhile, the MI didn't change and there was no gas consumption. However, it can be obviously found that the hydrate distribution still appeared inhomogeneity in sand sample.

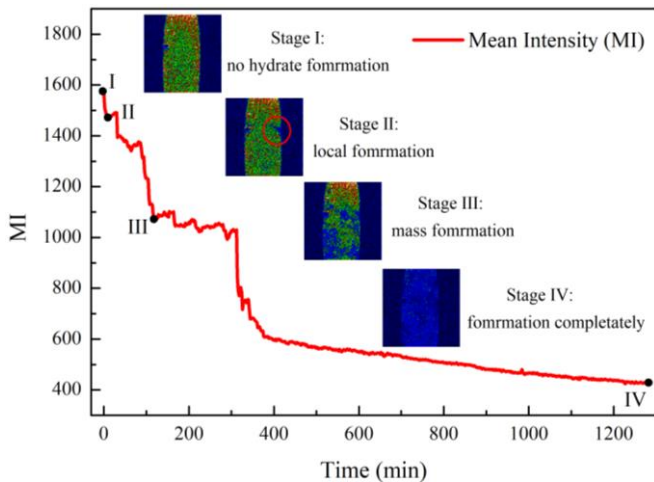


Fig. 2 The MI and water saturation distribution variations during hydrate formation

3.2 Visual observation of hydrate decomposition

Fig. 3 shows the water saturation distribution variations during hydrate decomposition process by the combination mode of water flow erosion and thermal simulation. The colors meaning in Fig. 3 are same as Fig. 2 in section 3.1. As obviously shown in Fig. 3, for all cases, the hydrate decomposition process can be classified to three stage: a) water saturation; b) residual gas displacement and suddenly hydrate formation/decomposition; c) continuous hydrate decomposition. Firstly, for stage I, plenty of free methane gas was continuously displaced by seawater, until the entire hydrate-bearing sand sample was saturated by seawater.

As shown, the image was more brighten for Case 3 than other two cases, which was caused by the higher seawater flow rate of 10mL/min. Then, the equilibrium stage of hydrate existing was suddenly broken due to the increase of chemical potential difference. Meanwhile, parts of hydrate decomposed at that moment, and the decomposition gas and residual gas in porous will be continually displaced by seawater. Therefore, there will be a phenomenon of the image variations from brighten to darken in stage II. What's more, doesn't exclude the

hydrate re-formation in stage II, which will also cause the darken of local region. For sage I and II, it's a shortly process. After the full saturation of hydrate-bearing sand sample, the whole image became brighten green due to the existing of residual porous and the hydrophilia of hydrate. Then, the phenomenon of obvious hydrate decomposition appeared as shown in stage III. It can be found that the seawater flow channel formed for all cases. Except for the difference that the one-side flow channel formed for Case 1 and 2 with the same flow rate of 2 mL/min, and middle flow channel formed for Case 3 with the flow rate of 10 mL/min. The similarity is that the hydrate gradually decomposed along the sides of flow channel for all cases. Finally, the whole FOV became brighten red when the hydrate decomposition completeness and the sand sample was fill with free water.

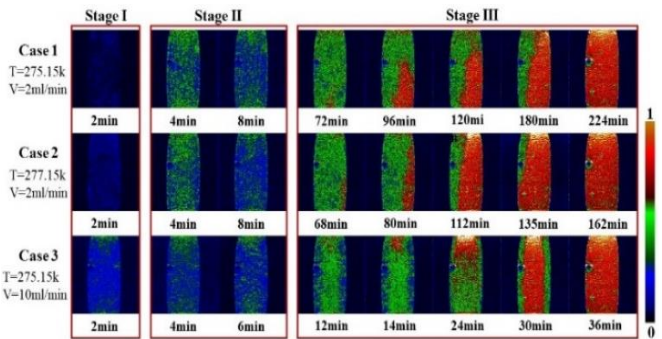


Fig. 3 The water saturation distribution variations during hydrate decomposition process by the combination mode of water flow erosion and thermal simulation

Fig. 4 shows the MI variations during hydrate decomposition process by the combination mode of water flow erosion and thermal simulation. It can be found that the MI for Case 3 was higher than Case 1 and 2 at point A. It was because the higher seawater flow rate of 10 mL/min for Case 3, which accelerated the saturation process. What's more, an obviously decrease of MI from point B to C. It's the stage II as described above, indicating that the decrease of free water saturation. After point C, the MI started to increase. Especially for Case 3, there was a rapidly increase trend of MI. The reason was that the seawater flow rate of 10 mL/min in this study will provide bigger drive force for hydrate decomposition than the seawater flow rate of 2 mL/min, though the temperature of flowing water for Case 3 was lower than Case 2. Compared with thermal simulation, this phenomenon also indicated that the chemical potential difference played a more important role on hydrate production. What's more, compare to

Case 1 and 2 (with the same seawater flow rate of 2 mL/min), there was a faster increase trend of Case 2 with the temperature of 277.15 K than Case 1 with the temperature of 275.15 K. The results indicated that there will be a bigger driving force for hydrate decomposition when the production temperature higher than the equilibrium pressure of hydrate. However, though the temperature of flowing seawater in Case 2 was higher than the hydrate-bearing sand sample, there will be still plenty of heat-loss during the flow process, which was inevitable. Therefore, the promotion effect of thermal simulation was not significant in this study. Even so, the thermal simulation method will induce the hydrate decomposition firstly. And then further increased the permeability for seawater flow process, avoiding the flow blockage as we found in our previous study [13].

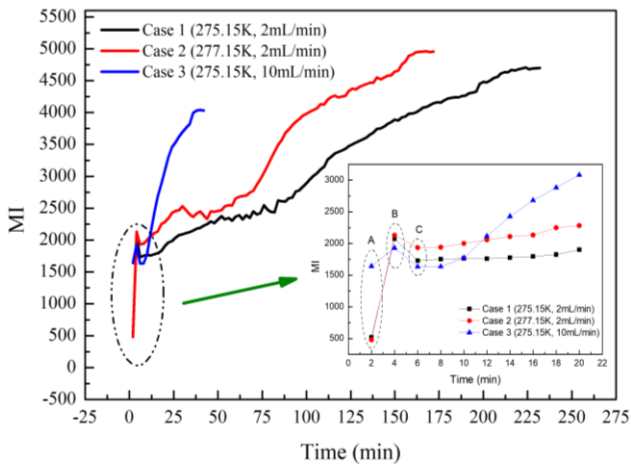


Fig. 4 The MI variations during hydrate decomposition process by the combination mode of water flow erosion and thermal simulation

3.3 Hydrate decomposition rate comparisons

MH decomposition rate is an important parameter for the evaluation of production method. Fig. 5 shows the variations of real-time MH decomposition rate and average MH decomposition rate. It can be found that the average decomposition of Case 2 with the higher temperature of flowing seawater, was little higher than Case 1. It indicated that the promotion effect of thermal simulation on hydrate decomposition. However, the plenty of heat-loss caused the unobvious differences of average decomposition rate between Case 1 and Case 2. For all cases, Case 3 with the temperature of 275.15 K and the seawater flow rate of 10 mL/min had the fastest average MH decomposition rate. In addition, the duration was also the shortest for Case 3. The results also indicated that the seawater flow played a more important role in the combination mode of seawater

flow erosion and thermal simulation, due to the plenty of heat-loss during flow process.

What's more, the real-time decomposition rate for Case 1 was relatively lower than other cases. However, the decomposition rate suddenly increased after 70 mins when the obvious hydrate decomposition appeared. And then the decomposition rate gradually tended to gentle after 140 mins when the seawater flow channel formed, due to the hydrate decomposition along the sides of flow channel. For Case 2, because of the higher temperature of flowing seawater, the fluctuation of real-time decomposition rate was relatively bigger than Case 1. The suddenly rise of decomposition rate was also appeared after the obvious hydrate decomposition appearing. For Case 3, the real-time decomposition rate gradually decrease with the hydrate decomposition until there was no hydrate existing in sand sample. The results also indicated that the bigger driving force improved by seawater flow. What's more, it can be found that the highest decomposition rate appeared at stage II (section 3.2) for Case 2 and 3, indicating that there must be parts of hydrate decomposition suddenly when the hydrate-bearing sand sample was saturated by seawater.

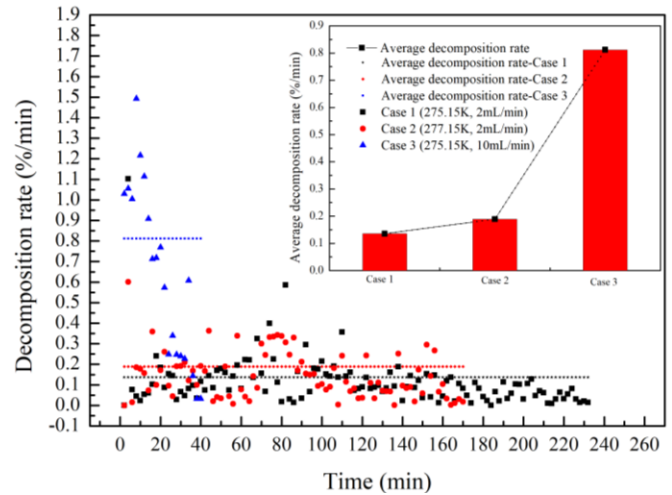


Fig. 4 The variations of real-time MH decomposition rate and average MH decomposition rate

4. CONCLUSION

In this study, a visualization investigation on the production characteristics of NGH by combination mode of thermal stimulation and water flow erosion in marine sediment was performed. According the conclusions as above, the results can be summarized as follow: (1) the combination mode will provide great decomposition driving force for hydrate with the higher temperature and seawater flow velocity. (2) there are three obvious stages for hydrate decomposition by the combination

mode: a) water saturation; b) residual gas displacement and sudden hydrate formation/ decomposition; c) hydrate decomposition. (3) the seawater flow process has more obvious promotion effect for hydrate decomposition than temperature increase. (4) the huge seawater source has great potential for actual hydrate production.

ACKNOWLEDGEMENT

This project was financially supported by the National Key Research and Development Plan of China (grant number 2017YFC0307303, 2016YFC0304001), the National Natural Science Foundation of China (grant number 51576025, 51436003), and the Fundamental Research Funds for the Central Universities of China.

REFERENCE

- [1] Song YC, Yang LL, Zhao JF, Liu WG, Yang MJ, Li Y, et al. The status of natural gas hydrate research in China: A review. *Renewable and Sustainable Energy Reviews*. 2014;31:778-91.
- [2] Li X-S, Xu C-G, Zhang Y, Ruan X-K, Li G, Wang Y. Investigation into gas production from natural gas hydrate: A review. *Applied Energy*. 2016;172:286-322.
- [3] Wang B, Fan Z, Wang P, Liu Y, Zhao J, Song Y. Analysis of depressurization mode on gas recovery from methane hydrate deposits and the concomitant ice generation. *Applied Energy*. 2017.
- [4] George J. Moridis MK. Depressurization-Induced Gas Production From Class 1 AND Class 2 Hydrate Deposits. Lawrence Berkeley National Laboratory. 2006.
- [5] Gao Y, Yang MJ, Zheng J-N, Chen BB. Production characteristics of two class water-excess methane hydrate deposits during depressurization. *Fuel*. 2018;232:99-107.
- [6] Reagan GJMMT. Strategies for Gas Production From Oceanic Class 3 Hydrate Accumulations. *SPE Journal*2007.
- [7] Chong ZR, Pujar GA, Yang M, Linga P. Methane hydrate formation in excess water simulating marine locations and the impact of thermal stimulation on energy recovery. *Applied Energy*. 2016;177:409-21.
- [8] Wang Y, Feng J-C, Li X-S, Zhang Y. Experimental and modeling analyses of scaling criteria for methane hydrate dissociation in sediment by depressurization. *Applied Energy*. 2016;181:299-309.
- [9] Lee J, Park S, Sung W. An experimental study on the productivity of dissociated gas from gas hydrate by depressurization scheme. *Energy Conversion and Management*. 2010;51:2510-5.

- [10] Xu C-G, Li X-S. Research progress on methane production from. *RCS advances*. 2018;5:54672-99.
- [11] Yang MJ, Fu Z, Zhao YC, Jiang LL, Zhao JF, Song YC. Effect of depressurization pressure on methane recovery from hydrate-gas-water bearing sediments. *Fuel*. 2016;166:419-26.
- [12] Chen BB, Yang MJ, Sun HR, Wang PF, Wang DY. Visualization study on the promotion of natural gas hydrate production by water flow erosion. *Fuel*. 2019;235:63-71.
- [13] Chen BB, Sun HR, Zhou H, Yang MJ, Wang DY. Effects of pressure and sea water flow on natural gas hydrate production characteristics in marine sediment. *Applied Energy*. 2019;238:274-83.
- [14] Sean W-Y, Sato T, Yamasaki A, Kiyono F. CFD and experimental study on methane hydrate dissociation Part I. Dissociation under water flow. *AIChE Journal*. 2007;53:262-74.
- [15] Chong ZR, Yang SHB, Babu P, Linga P, Li X-S. Review of natural gas hydrates as an energy resource: Prospects and challenges. *Applied Energy*. 2016;162:1633-52.